energies

MDPI

Article

Demand Aware Dynamic Pricing for Smart Grid Communication Networks: A Stackelberg Game Approach

Xingxing Feng [1], Haitong Gu [1], Bin Guo [1], Xiaoqiang Wu [1], Jun Dong [1], Jingbo Lin [1], Weidong Wang [2,*] and Quansheng Guan [2]

1 Guangzhou Power Supply Bureau, Guangdong Power Grid Co., Ltd., Guangzhou 510620, China; xingxfing@163.com (X.F.); 13822100718@139.com (H.G.); guobin735000@163.com (B.G.); wuxq999@126.com (X.W.); dojundong@163.com (J.D.); jingblin@163.com (J.L.)

2 School of Electronic and Information Engineering, South China University of Technology, 381 Wushan Road, Guangzhou 510640, China; eeqshguan@scut.edu.cn

* Correspondence: acwweidwang@163.com

Abstract

Smart grid communication services often have heterogeneous and time-varying bandwidth demands, which makes fixed resource allocation and flat pricing less suitable for on-demand service provisioning. This paper studies a demand-aware dynamic pricing problem in a resource-allocable communication network enabled by software-defined networking, where service requests observe network resource status and purchase bandwidth according to the announced price. Unlike pricing models that mainly describe the price–quantity tradeoff, the proposed model incorporates the minimum acceptable bandwidth demand of each request as a service-side acceptance threshold. A Stackelberg game is formulated in which the communication resource manager acts as the leader and service requests act as followers. We define the utility and revenue functions, analyze the existence of equilibrium, and derive the follower-side best response through backward induction. The resulting response is piecewise, which makes exact equilibrium characterization difficult in multi-user settings. Therefore, a distributed iterative algorithm and a backward-induction-based genetic algorithm are developed for different information settings. Simulation results show how service-side parameters affect pricing behavior and evaluate the proposed methods under heterogeneous-user, multi-user, and capacity-limited scenarios.

Keywords: smart grid communication; software-defined networking; Stackelberg game

1. Introduction

Communication networks are increasingly expected to support service requests with heterogeneous and time-varying bandwidth demands [1]. In many practical systems, however, communication resources are still provisioned in a relatively fixed manner, where bandwidth is allocated according to predefined plans or long-term service agreements. Although this provisioning mode is easy to manage, it is inefficient when demand varies with time and operating conditions. It may cause resource under-utilization under light demand and insufficient support under rapidly increasing demand, which is relevant to flexible service provisioning in smart grid-motivated communication scenarios [2,3]. Resource-constrained and sensing-enabled Internet-of-Things systems also highlight the need for adaptive communication resource management in dynamic environments [4].

Software-defined networking (SDN) provides a feasible technical basis for more flexible resource management by separating the control plane from the data plane and enabling

Check for updates

Academic Editor: Michael Negnevitsky

Received: 2 May 2026
Revised: 2 June 2026
Accepted: 4 June 2026
Published: 15 June 2026

programmable network control [5,6]. With SDN support, a resource-allocable communication network can expose resource status information to upper-layer service requests and support on-demand bandwidth provisioning [7]. In such a scenario, service requests can observe candidate paths, communication delay, residual bandwidth, and unit price, and then submit bandwidth requests according to their current needs [8]. Compared with one-size-fits-all provisioning, this mechanism better matches communication resources with dynamic service demands. However, it does not answer how the communication resource manager should price resources when service-side demand is price-sensitive.

Existing studies on SDN-enabled communication resource management have investigated dynamic path selection, bandwidth scheduling, traffic engineering, and quality of service (QoS)/quality of experience (QoE)-aware resource allocation [9–13]. These works have substantially improved the flexibility of resource provisioning and have laid an important foundation for resource-allocable communication networks [7]. However, most of them primarily address how to allocate or schedule resources efficiently after the demand is given, rather than how to determine prices when service requests adjust their demand in response to the announced price. As a result, the interaction between pricing decisions and service-side demand behavior is still insufficiently characterized in many resource-allocation-oriented studies.

In parallel, extensive research has addressed network pricing and bandwidth pricing from economic and optimization perspectives [14]. Representative approaches include flat-rate pricing, usage-based pricing, auction-based pricing, and game-theoretic pricing [15,16]. Among these, Stackelberg-game-based models are widely used to describe the interaction between a resource provider and its users, where the provider announces the price and users respond by choosing their resource demands. Although these studies provide useful pricing tools, many formulations remain provider-oriented. User demand is often modeled through the price–quantity tradeoff, while the minimum acceptable service demand is simplified or ignored. In service-oriented communication scenarios, however, a request may reject an allocation that fails to satisfy its minimum bandwidth requirement. Thus, incorporating the minimum acceptable bandwidth demand into the utility model helps characterize both service-side acceptance behavior and provider-side pricing decisions.

Motivated by this observation, this paper studies a demand-aware dynamic pricing problem in an SDN-enabled resource-allocable communication network under a smart grid motivated application context. A communication resource manager provides bandwidth resources to multiple service requests. The manager first announces the unit bandwidth price, and each service request then determines its purchased bandwidth by maximizing its own utility. Different from conventional models that only capture the tradeoff between price and purchased amount, the proposed formulation explicitly incorporates the minimum acceptable bandwidth demand of each service request. In this way, the model can reflect a basic acceptance constraint in communication services: bandwidth allocation is meaningful only when the purchased resource satisfies the minimum service requirement [17].

To characterize the interaction between the communication resource manager and multiple service requests, this paper formulates the pricing problem as a Stackelberg game. The communication resource manager acts as the leader and determines the unit bandwidth price, while service requests act as followers and choose their purchased bandwidth to maximize individual utilities. On this basis, we analyze equilibrium existence and derive the follower-side response through backward induction. Because the minimum acceptable demand makes the response piecewise across parameter regions, exact equilibrium characterization becomes difficult in multi-user scenarios. We therefore develop a distributed iterative algorithm and a backward-induction-based genetic algorithm for different information settings [18,19]. The main contributions of this paper can be summarized as follows.

- A demand-aware dynamic pricing problem is formulated for an SDN-enabled resource-allocable communication network. In the considered scenario, service requests can observe path, delay, residual bandwidth, and unit price information, and request bandwidth resources on demand.
- A Stackelberg game-based pricing model is proposed by explicitly incorporating the minimum acceptable bandwidth demand into the utility function of each service request. Different from conventional Stackelberg pricing models that mainly characterize a continuous price–quantity response, the proposed formulation treats the minimum acceptable bandwidth demand as a service-side admission threshold. This enables the model to capture both service-side acceptance behavior and provider-side pricing decisions.
- The existence of the equilibrium is analyzed, and the follower-side response is derived through backward induction. Since the resulting response becomes piecewise and difficult to solve exactly in multi-user scenarios, a distributed iterative algorithm and a backward-induction-based genetic algorithm are developed to obtain approximate solutions. Simulation studies are conducted to reveal the impacts of service-side parameters on pricing behavior and to validate the proposed methods under heterogeneous-user, multi-user, and capacity-limited scenarios.

The remainder of this paper is organized as follows. Section 2 reviews related work on dynamic resource allocation, bandwidth pricing, and Stackelberg game-based pricing methods. Section 3 describes the system scenario and formulates the demand-aware pricing problem. Section 4 presents the Stackelberg game model. Section 5 analyzes the equilibrium properties. Section 6 introduces the proposed solution algorithms. Section 7 reports the simulation results and discussion. Finally, Section 8 concludes the paper.

2. Related Work

SDN-based dynamic resource allocation: The programmability of SDN has enabled extensive research on dynamic communication resource allocation [5–7]. Existing studies have investigated dynamic path selection, traffic engineering, bandwidth scheduling, and QoS/QoE-aware resource management in programmable networks [9–13]. These efforts have shown that network status can be monitored in real time and that allocation decisions can be updated online according to network conditions and service requirements. They therefore provide the technical foundation for resource-allocable communication networks, in which service requests can observe network status and request communication resources on demand [8]. Related studies have also explored exposing limited control or customization capability to end users and applications in SDN environments, so that service intent can be expressed more directly from the user side [20–22]. However, this line of work mainly focuses on allocation efficiency, routing flexibility, or service quality improvement under given demand, while the interaction between pricing decisions and service-side demand response is rarely modeled explicitly.

Network pricing and bandwidth pricing: In parallel with resource-allocation-oriented research, extensive studies have investigated pricing mechanisms for communication and network resources [14]. Early approaches mainly adopted static pricing schemes, such as flat-rate pricing and usage-based pricing, because of their operational simplicity. To improve resource utilization and adapt to demand variation, subsequent studies considered dynamic pricing, differentiated pricing, and auction-based pricing mechanisms [15]. In application-driven communication scenarios, some work further incorporated service characteristics, traffic load, link capacity, or QoS-related factors into the pricing process in order to better match price with resource demand [23,24]. Nevertheless, in many pricing models, the demand side is still represented in a simplified manner. In particular, user response is usually characterized as a price–quantity relationship, where the purchased bandwidth changes continuously with the announced price. The service-side acceptance threshold, namely, the minimum bandwidth level below which the allocation is not useful to the request, is not explicitly modeled. This limitation motivates the demand-aware pricing model developed in this paper, in which the minimum acceptable bandwidth demand is incorporated into the utility function and further affects the follower-side response.

Game-theoretic pricing and Stackelberg models: Game theory has become an important tool for modeling the interaction between resource providers and demanders in communication networks [16]. Among different formulations, Stackelberg games are suitable for pricing problems because they describe the sequential process in which the provider first sets the price and users then decide their resource demands. Existing studies have applied Stackelberg models to bandwidth pricing, cloud service pricing, edge resource trading, and related allocation problems [16,25]. Some studies derive exact equilibrium solutions, while others develop approximate algorithms when closed-form analysis is difficult [25,26]. However, many existing models remain provider-oriented and treat user response as a continuous reaction to price. In service-oriented communication scenarios, this assumption may be insufficient because a request may reject an allocation that does not meet its minimum acceptable bandwidth requirement [17].

Taken together, the existing literature still leaves three gaps. First, many SDN-based studies focus on dynamic allocation under exogenously given demand, rather than demand-aware pricing. Second, many network pricing models do not explicitly incorporate the minimum acceptable bandwidth demand of service requests. Third, existing Stackelberg pricing studies are seldom discussed in a resource-allocable communication setting, where service requests can observe network status and request bandwidth on demand. These gaps are particularly relevant for application-motivated communication scenarios, including smart grid-motivated ones, and they motivate the demand-aware dynamic pricing model developed in this paper [1,3].

3. System Scenario and Problem Formulation

3.1. System Scenario

We consider an SDN-enabled resource-allocable communication network motivated by smart grid service scenarios. A communication resource manager controls network resources and serves multiple service requests with heterogeneous and time-varying bandwidth demands. In this paper, the smart grid context is used as an application-motivated communication scenario, and the proposed model mainly captures communication-side characteristics such as heterogeneous service demands, time-varying bandwidth requirements, and minimum acceptable bandwidth levels for service admission.

The key feature of the considered network is that service requests can observe selected network-state information and request bandwidth on demand. Specifically, the control plane exposes candidate paths, communication delay, residual bandwidth, and unit price, while the manager performs resource provisioning based on the global network view [5–8].

As shown in Figure 1, the network extends the conventional SDN architecture with an explicit interaction interface for upper-layer service requests. This allows demand expression to be coupled with resource visibility, rather than being restricted to predefined service plans.

Figure 2 shows the operational view of this scenario. The SDN controller is responsible for network monitoring, customization, and routing. It collects topology and resource-state information from the data plane and supports path-aware bandwidth provisioning through the control plane. This setting provides the system basis for subsequent pricing decisions. It should be noted that the communication resource manager is not assumed to have unlimited computational capability or perfect knowledge of future network states. The model assumes that, within each pricing interval, the SDN controller can obtain sufficiently updated information on candidate paths, delay, residual bandwidth, and capacity through network monitoring. These network states are treated as quasi-static during one pricing interval. Delayed or inaccurate state information may affect the estimation of feasible resources and thus lead to a mismatch between the announced price and the actual available bandwidth. However, this issue affects the accuracy of the input information rather than the basic Stackelberg structure of the pricing model.

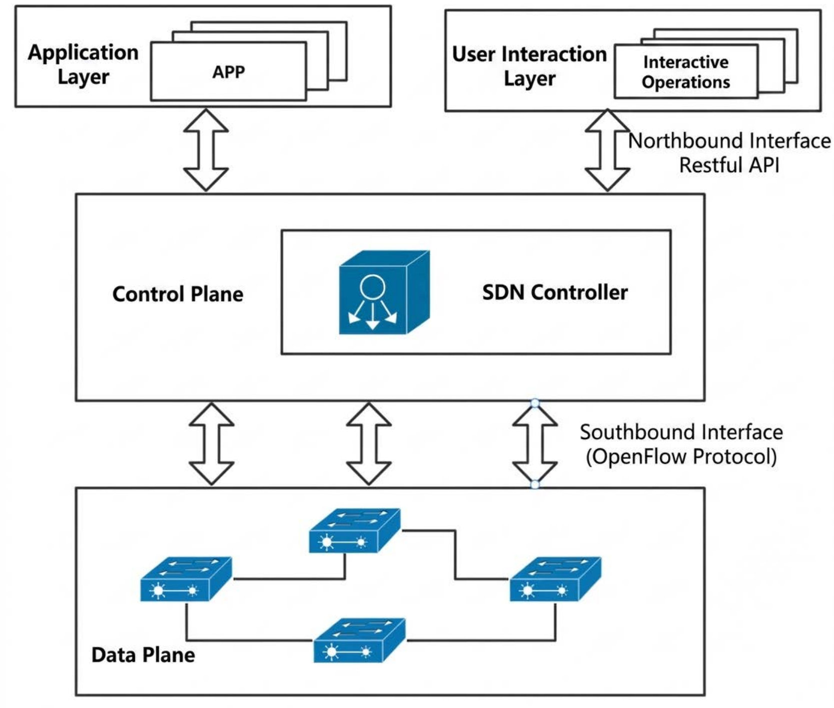

Figure 1. Architecture of the SDN-enabled resource-allocable communication network.

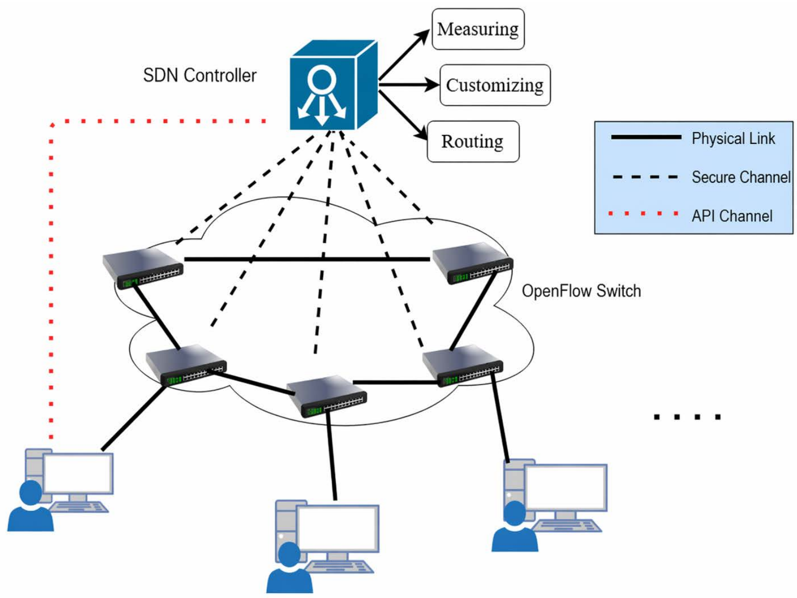

Figure 2. Operational view of the resource-allocable communication scenario.

Accordingly, the provider recomputes the price on a pricing-interval basis rather than continuously for every packet-level network variation. The length of the pricing interval should be selected according to the variation speed of residual bandwidth, service demand, and admission conditions. In a relatively stable network state, a longer pricing interval can reduce computational and signaling overhead. When the observed resource state or service demand changes significantly, a shorter interval or event-triggered price recomputation can be adopted. Therefore, the recomputation frequency is an implementation parameter that balances pricing responsiveness and control overhead, rather than a fixed value imposed by the theoretical model.

3.2. Pricing-Oriented Abstraction

Based on the above scenario, we abstract the communication process into a pricing-oriented decision model. Let $\mathcal{I} = \{1, 2, \ldots, N\}$ denote the set of service requests. During each pricing interval, the communication resource manager announces a price p, and each service request $i \in \mathcal{I}$ determines its purchased bandwidth b_i according to its own utility.

Each service request is associated with a minimum acceptable bandwidth demand, denoted by B_i. This parameter represents a service-side admission threshold rather than a hard obligation to purchase bandwidth. If service request i decides to purchase bandwidth, the purchased amount must satisfy $b_i \geq B_i$; otherwise, the request may choose $b_i = 0$, which indicates non-participation or service rejection. Thus, a positive bandwidth purchase is meaningful only when it reaches the minimum acceptable bandwidth demand. In addition, E_i denotes the maximum attainable benefit of service request i when price is not considered, and r_i characterizes the return of additional bandwidth beyond the minimum acceptable demand. These parameters capture heterogeneous service-side benefit patterns under bandwidth provisioning. Multiple service classes are not explicitly indexed in the current model, but their heterogeneous bandwidth requirements can be reflected through different settings of B_i, E_i, and r_i; explicit QoS-priority modeling is left for future work.

Although path and delay information do not explicitly appear in the core variables $\{p, b_i, B_i, E_i, r_i\}$, they remain relevant in the system. Their role is to determine which communication option is feasible and visible to a service request, while the subsequent pricing model focuses on the bandwidth-purchase decision after a feasible option has been identified.

3.3. Problem Formulation

The problem considered in this paper is to determine a pricing decision that coordinates provider-side revenue and service-side acceptance in the above resource-allocable communication scenario. The communication resource manager determines the price p, while each service request chooses b_i in response to the announced price and accepts the allocation only when its minimum requirement is satisfied in a meaningful way.

Because the manager moves first and service requests respond afterward, the interaction naturally forms a leader–follower structure. This motivates a Stackelberg formulation, in which the manager acts as the leader and the service requests act as followers. Under this formulation, p is the announced unit bandwidth price, b_i is the purchased bandwidth, B_i is the minimum acceptable demand, E_i is the maximum attainable benefit, and r_i is the return factor of additional bandwidth. The formal utility and revenue models are introduced in the next section.

4. Stackelberg Game-Based Pricing Model

This section formulates the demand-aware pricing problem as a Stackelberg game. We consider one communication resource manager and N service requests in the SDN-enabled resource-allocable communication network described in Section 3. The manager announces a unit bandwidth price, and each service request determines its purchased bandwidth in response to that price. We first consider the case where the aggregate demand induced by the announced price can be satisfied. The capacity-limited case will be discussed later in Section 7.

4.1. Model Definition

Let $\mathcal{I} = \{1, 2, \ldots, N\}$ denote the set of service requests. The communication resource manager acts as the leader and determines the unit bandwidth price p, where $p > 0$. Each service request $i \in \mathcal{I}$ acts as a follower and chooses its purchased bandwidth b_i after observing the announced price. The main notation is summarized in Table 1.

Table 1. Main notation used in the pricing model.

Symbol	Description
$\mathcal{I}$	Set of service requests, $\mathcal{I} = \{1, 2, \ldots, N\}$
p	Unit bandwidth price announced by the communication resource manager
b_i	Purchased bandwidth of service request i under price p
B_i	Minimum acceptable bandwidth demand of service request i
E_i	Maximum attainable benefit of service request i when price is not considered
r_i	Return factor of additional bandwidth beyond B_i, where $r_i \in (0, 1]$
U_i	Utility of service request i
R	Revenue of the communication resource manager

In this model, B_i represents the minimum acceptable bandwidth demand that must be satisfied before a bandwidth purchase becomes meaningful to service request i. The parameter E_i captures the upper bound of the service-side benefit, while r_i characterizes the return of additional bandwidth beyond the minimum acceptable bandwidth demand. Therefore, (B_i, E_i, r_i) jointly characterizes the service-side demand and benefit profile of request i.

4.2. Utility and Revenue Functions

The utility of service request i is designed to satisfy three requirements. First, the request should have an explicit minimum acceptable bandwidth demand. Second, the service-side benefit should be bounded above. Third, additional bandwidth beyond the minimum acceptable bandwidth demand should yield heterogeneous returns across different requests.

Based on these considerations, the utility of service request i is defined as

$$U_i(b_i, p) = \frac{E_i}{1 + e^{r_i(B_i - b_i)}} - pb_i, \qquad b_i \geq B_i. \tag{1}$$

For clarity, (1) can be decomposed into a benefit term and a payment term:

$$u_i(b_i) = \frac{E_i}{1 + e^{r_i(B_i - b_i)}}, \tag{2}$$

$$c_i(b_i, p) = pb_i, \tag{3}$$

and

$$U_i(b_i, p) = u_i(b_i) - c_i(b_i, p). \tag{4}$$

The function in (2) is upper-bounded by E_i, which means that the service-side benefit cannot increase without limit as bandwidth grows. The shifted sigmoid form is adopted as a tractable satisfaction model for bandwidth provisioning rather than as an empirically fitted traffic-demand law. This choice is motivated by the observation that the perceived benefit of additional bandwidth is usually nonlinear: it increases rapidly around the minimum service requirement but gradually saturates after the service demand is sufficiently satisfied. By shifting the sigmoid function with B_i, the main transition region of the benefit function is placed around the minimum acceptable bandwidth demand, so that B_i can explicitly represent the service-side admission threshold. Meanwhile, r_i controls the steepness of this transition and therefore characterizes heterogeneous sensitivity to additional bandwidth among different service requests.

Compared with several common alternatives, the shifted sigmoid utility function better matches the modeling objective of this work. A linear utility function cannot describe benefit saturation, while a logarithmic utility function captures diminishing marginal benefit but does not explicitly place the satisfaction transition around a minimum acceptable bandwidth threshold. The α-fair utility function is mainly used for fairness-oriented resource allocation, whereas this work focuses on service-side admission behavior under price-sensitive bandwidth purchasing.

If no non-negative utility can be obtained over the feasible region $b_i \geq B_i$, then service request i does not purchase bandwidth, i.e.,

$$b_i = 0. \tag{5}$$

The revenue of the communication resource manager is defined as

$$R(p, \mathbf{b}) = p \sum_{i \in \mathcal{I}} b_i, \tag{6}$$

where $\mathbf{b} = (b_1, b_2, \ldots, b_N)$ is the bandwidth-demand vector of all service requests. In this paper, $R(p, \mathbf{b})$ represents the gross revenue of the communication resource manager. Operational costs, congestion costs, fairness terms, and QoS penalties are not explicitly included in the objective function, because the present work focuses on the demand-aware pricing response between the manager and service requests. These factors can be incorporated as additional cost or penalty terms in an extended cost-aware or QoS-aware pricing model.

4.3. Stackelberg Formulation

The above interaction is modeled as a Stackelberg game. The communication resource manager acts as the leader and determines the unit bandwidth price p. Each service request acts as a follower and chooses its purchased bandwidth by solving

$$\max_{b_i} U_i(b_i, p) \quad \text{s.t.} \quad b_i \geq B_i, \tag{7}$$

when it participates in bandwidth purchasing. If the resulting maximum utility over $b_i \geq B_i$ is negative, the service request selects $b_i = 0$, which represents non-participation rather than a bandwidth allocation below the minimum acceptable demand. Equivalently, the effective decision set is $\{0\} \cup [B_i, \infty)$. The rational response assumption is used as a modeling abstraction for service requests or application-side controllers that adjust bandwidth demand according to predefined cost–benefit rules.

Accordingly, the communication resource manager solves

$$\max_{p > 0} \; R\big(p, \mathbf{b}(p)\big), \tag{8}$$

where $\mathbf{b}(p)$ denotes the follower-side demand response induced by the announced price.

This formulation highlights the key feature of the proposed model: each service

https://doi.org/10.3390/en19122846

request responds not only to price but also to its minimum acceptable bandwidth demand. The equilibrium properties of the proposed game and the structure of the follower-side response are analyzed in the next section.

5. Equilibrium Analysis

In this section, we analyze the equilibrium properties of the proposed Stackelberg game. We first show that, for a given price, each follower admits a well-defined optimal response. We then derive the follower-side best response by backward induction and show that the resulting demand function is piecewise. This piecewise structure makes it difficult to obtain a closed-form exact equilibrium in the multi-request case, thereby motivating the approximate algorithms presented in the next section.

5.1. Existence of Equilibrium

For a given price p, the utility of service request i is

$$U_i(b_i, p) = \frac{E_i}{1 + e^{r_i(B_i - b_i)}} - pb_i, \qquad b_i \geq B_i. \tag{9}$$

Its first derivative with respect to b_i is

$$\frac{\partial U_i}{\partial b_i} = \frac{E_i r_i e^{r_i(B_i - b_i)}}{\left(1 + e^{r_i(B_i - b_i)}\right)^2} - p, \tag{10}$$

and the second derivative is

$$\frac{\partial^2 U_i}{\partial b_i^2} = \frac{E_i r_i^2 e^{r_i(B_i - b_i)}\left(e^{r_i(B_i - b_i)} - 1\right)}{\left(1 + e^{r_i(B_i - b_i)}\right)^3}. \tag{11}$$

Since $b_i \geq B_i$, we have $e^{r_i(B_i - b_i)} \leq 1$, and therefore

$$\frac{\partial^2 U_i}{\partial b_i^2} \leq 0. \tag{12}$$

Hence, $U_i(b_i, p)$ is concave over the feasible region $b_i \geq B_i$. Therefore, for any given price p, the follower-side problem admits an optimal solution. If the maximum utility over $b_i \geq B_i$ is negative, service request i chooses not to purchase bandwidth, i.e., $b_i = 0$. Otherwise, it chooses the unique maximizer over the feasible region.

Based on the above result, let $b_i^*(p)$ denote the best response of service request i under price p, and let

$$\mathbf{b}^*(p) = \left(b_1^*(p), b_2^*(p), \ldots, b_N^*(p)\right) \tag{13}$$

denote the follower-side response vector. The leader-side revenue is then

$$R\left(p, \mathbf{b}^*(p)\right) = p \sum_{i \in \mathcal{I}} b_i^*(p). \tag{14}$$

Moreover, for each service request i, the utility decreases with price since

$$\frac{\partial U_i}{\partial p} = -b_i \leq 0. \tag{15}$$

The Stackelberg equilibrium can be stated through the standard leader–follower optimality conditions. For any given price $p > 0$, each service request chooses a best response over the effective decision set $\{0\} \cup [B_i, \infty)$, where $b_i = 0$ represents non-participation.

Since $U_i(b_i, p)$ is continuous over $b_i \geq B_i$, concave over the feasible purchase region, and decreases to negative values as b_i becomes sufficiently large due to the linear payment term, the follower-side best response exists for any announced price.

On the leader side, the service-side benefit is upper-bounded by E_i. Therefore, if $p > E_i/B_i$, then $U_i(b_i, p) \leq E_i - pB_i < 0$ for all $b_i \geq B_i$, and service request i chooses $b_i = 0$. Hence, the provider-side search can be restricted to a bounded price interval, for example, $p \in (0, \bar{p}]$, where

$$\bar{p} = \max_{i \in \mathcal{I}} \frac{E_i}{B_i}. \tag{16}$$

Within this bounded interval, the follower-side response is piecewise continuous with a finite number of threshold points because the number of service requests is finite. As a result, the leader-side revenue

$$R(p, \mathbf{b}^*(p)) = p \sum_{i \in \mathcal{I}} b_i^*(p) \tag{17}$$

attains at least one maximum over the corresponding piecewise-defined regions. Let p^* denote such a revenue-maximizing price and let $\mathbf{b}^* = \mathbf{b}^*(p^*)$ be the induced follower response. Then, each follower maximizes its own utility under p^*, and the leader maximizes its revenue given the followers' best responses. Therefore, $(p^*, \mathbf{b}^*)$ constitutes a Stackelberg equilibrium of the proposed game.

5.2. Backward Induction-Based Analysis

We now derive the follower-side best response under a given price p. For convenience, we first consider the benefit term

$$u_i(b_i) = \frac{E_i}{1 + e^{r_i(B_i - b_i)}}, \tag{18}$$

whose first derivative is

$$\frac{\partial u_i}{\partial b_i} = \frac{E_i r_i e^{r_i(B_i - b_i)}}{\left(1 + e^{r_i(B_i - b_i)}\right)^2}. \tag{19}$$

Since $u_i(b_i)$ is concave over $b_i \geq B_i$, the derivative in (19) attains its maximum at $b_i = B_i$. Define

$$p_i^{\max} = \left.\frac{\partial u_i}{\partial b_i}\right|_{b_i = B_i} = \frac{E_i r_i}{4}. \tag{20}$$

Figure 3 provides a qualitative illustration of the marginal benefit under the proposed utility model. It shows that the marginal benefit decreases as bandwidth increases and that different parameter settings may lead to different decay patterns.

Equation (20) represents the largest marginal benefit that service request i can obtain from bandwidth purchase. Therefore, if

$$p \geq p_i^{\max}, \tag{21}$$

the payment slope dominates the marginal utility over the feasible region, and $U_i(b_i, p)$ becomes nonincreasing for all $b_i \geq B_i$. In this case, the best feasible purchase, if accepted, is attained at $b_i = B_i$. Since

$$U_i(B_i, p) = \frac{E_i}{2} - pB_i, \tag{22}$$

the corresponding acceptance threshold is defined as

$$\hat{p}_i = \frac{E_i}{2B_i}. \tag{23}$$

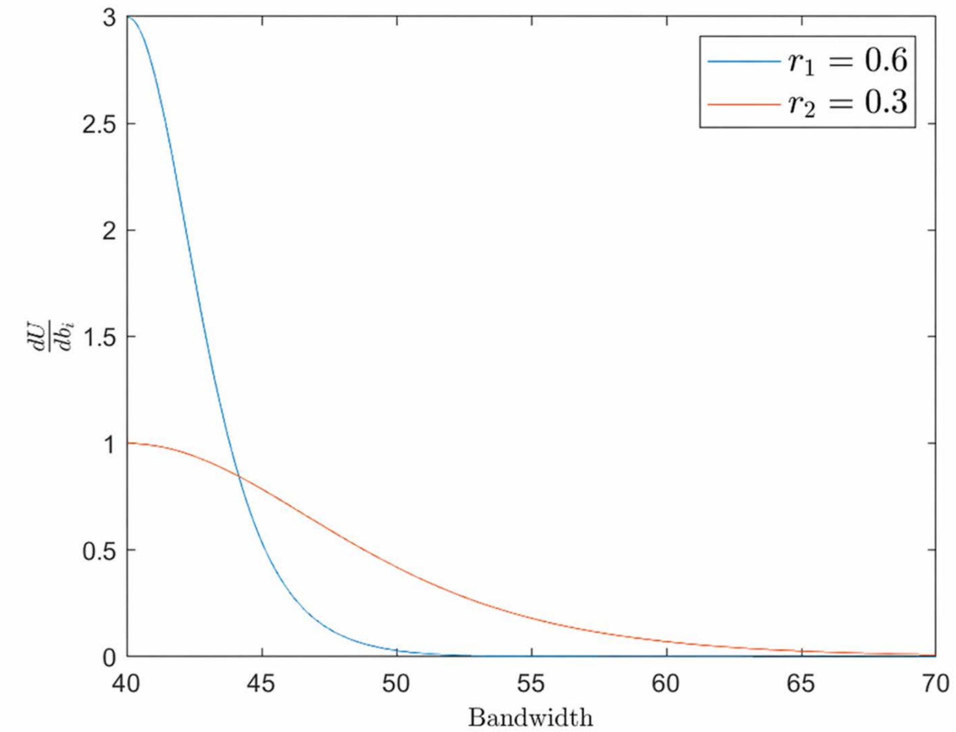

Figure 3. Qualitative illustration of the marginal benefit of bandwidth under the proposed utility model for two illustrative settings with $r_1 = 0.6$ and $r_2 = 0.3$.

Thus, when $p \geq p_i^{\max}$,

$$b_i^*(p) = \begin{cases} B_i, & p \leq \hat{p}_i, \\ 0, & p > \hat{p}_i. \end{cases} \tag{24}$$

We next consider the case

$$0 < p < p_i^{\max}. \tag{25}$$

Setting (10) to zero gives the first-order condition

$$\frac{E_i r_i e^{r_i(B_i - b_i)}}{\left(1 + e^{r_i(B_i - b_i)}\right)^2} = p. \tag{26}$$

Let

$$x_i = e^{r_i(B_i - b_i)}. \tag{27}$$

Then, (26) becomes

$$p x_i^2 + (2p - E_i r_i) x_i + p = 0. \tag{28}$$

The two roots are

$$x_{i,1} = \frac{E_i r_i - 2p + \sqrt{E_i r_i (E_i r_i - 4p)}}{2p}, \tag{29}$$

$$x_{i,2} = \frac{E_i r_i - 2p - \sqrt{E_i r_i (E_i r_i - 4p)}}{2p}. \tag{30}$$

Because $b_i \geq B_i$ implies $x_i \leq 1$, the feasible interior solution is obtained from $x_{i,2}$. Hence, the interior candidate is

$$\tilde{b}_i(p) = B_i - \frac{1}{r_i} \ln\left(\frac{E_i r_i - 2p - \sqrt{E_i r_i (E_i r_i - 4p)}}{2p} \right). \tag{31}$$

Substituting (31) into (9), the corresponding utility is

$$U_i\big(\tilde{b}_i(p), p\big) = \frac{E_i}{1 + x_{i,2}} - p\left(B_i - \frac{1}{r_i}\ln x_{i,2}\right), \tag{32}$$

where $x_{i,2}$ is given by (30).

At this point, the follower-side response becomes piecewise according to the relation between B_i and r_i.

5.2.1. Case 1: $B_i r_i \le 2$

When $B_i r_i \le 2$, we have $\hat{p}_i \ge p_i^{\max}$. In this case, the utility at the feasible optimum remains non-negative up to the boundary price $p_i^{\max}$, and no additional zero-utility threshold is needed. Therefore, the best response is

$$b_i^*(p) = \begin{cases} 0, & p > \hat{p}_i, \\ B_i, & p_i^{\max} \le p \le \hat{p}_i, \\ \tilde{b}_i(p), & 0 < p < p_i^{\max}. \end{cases} \tag{33}$$

5.2.2. Case 2: $B_i r_i > 2$

When $B_i r_i > 2$, the utility at the boundary point $b_i = B_i$ becomes negative before p reaches $p_i^{\max}$. In this case, there exists a threshold

$$p_i^{\text{zero}} \in (0, p_i^{\max}) \tag{34}$$

such that

$$U_i\big(\tilde{b}_i(p_i^{\text{zero}}), p_i^{\text{zero}}\big) = 0. \tag{35}$$

Hence, the best response becomes

$$b_i^*(p) = \begin{cases} 0, & p > p_i^{\text{zero}}, \\ \tilde{b}_i(p), & 0 < p \le p_i^{\text{zero}}. \end{cases} \tag{36}$$

Equations (33) and (36) show that the follower-side response is a piecewise function jointly determined by the price and the service-side parameters. In particular, the minimum acceptable bandwidth demand B_i plays a decisive role in shaping the response region.

Substituting the follower-side response into the leader-side objective yields

$$R\big(p, \mathbf{b}^*(p)\big) = p \sum_{i \in \mathcal{I}} b_i^*(p), \tag{37}$$

which is a multi-segment function under heterogeneous service parameters. Since each service request contributes only a finite number of price thresholds, the number of price segments grows at most linearly with the number of service requests. As the number of service requests increases, the segmentation structure becomes increasingly complicated, and a direct closed-form exact equilibrium is difficult to obtain. For this reason, the next section develops approximate solution algorithms for different scenarios.

6. Solution Algorithms

As shown in Section 5, the follower-side best response is piecewise-defined, and the leader-side revenue

$$R\big(p, \mathbf{b}^*(p)\big) = p \sum_{i \in \mathcal{I}} b_i^*(p) \tag{38}$$

becomes a multi-segment function with heterogeneous threshold points across service requests. In multi-user scenarios, directly characterizing the exact equilibrium in closed form is difficult. For this reason, this section develops two approximate solution methods for different information settings.

When service requests do not reveal their utility parameters, the communication resource manager cannot directly evaluate the response function in Section 5. In this case, a distributed iterative algorithm is used. When the manager can obtain the service-side parameters and compute follower responses through backward induction, a genetic algorithm is adopted to search for a more accurate approximate equilibrium.

6.1. Distributed Iterative Algorithm

The distributed iterative algorithm is designed for privacy-sensitive settings in which the communication resource manager does not know the detailed utility parameters of individual service requests. The manager only announces a price, collects the bandwidth responses returned by service requests, and updates the price iteratively.

Let $\lambda > 0$ denote the price step size. Starting from an initial price $p^{(0)} = \lambda$, the manager broadcasts the current price $p^{(t)}$ to all service requests. Each service request computes its best response $b_i^*(p^{(t)})$ according to the piecewise expressions derived in Section 5 and feeds the result back to the manager. After receiving all responses, the manager computes the revenue

$$R^{(t)} = p^{(t)} \sum_{i \in \mathcal{I}} b_i^*(p^{(t)}), \tag{39}$$

stores the current price–response pair, and then updates the price as

$$p^{(t+1)} = p^{(t)} + \lambda. \tag{40}$$

The procedure terminates when all service requests reject the current price, i.e.,

$$\mathbf{b}^*(p^{(t)}) = (0, \ldots, 0), \tag{41}$$

or when a prescribed iteration limit is reached. The final approximate solution is selected from the recorded history as

$$p^\dagger = \arg\max_t R^{(t)}, \qquad \mathbf{b}^\dagger = \mathbf{b}^*(p^\dagger). \tag{42}$$

The above procedure terminates in finite time for any $\lambda > 0$, because the follower-side demand eventually vanishes as the announced price exceeds the effective acceptance range derived in Section 5. Therefore, after a finite number of updates, the algorithm reaches a price at which no service request purchases bandwidth, and the best recorded historical solution is returned. The procedure of the distributed iterative algorithm is summarized in Algorithm 1.

In Step 3 of Algorithm 1, each service request computes its bandwidth response under the announced price based on its own service-side parameters and the best-response results derived in Section 5. Specifically, service request i first identifies the applicable response case according to the relationship among B_i, r_i, and the relevant price thresholds, including $p_i^{\max}$, $\hat{p}_i$, and, when applicable, p_i^{zero}. It then returns the corresponding bandwidth demand, which may be $\tilde{b}_i(p^{(t)})$, B_i, or zero. If the maximum utility over the feasible region $b_i \geq B_i$ is negative, the service request returns zero demand, indicating that it does not purchase bandwidth at the current price. After collecting the responses from all service requests, the communication resource manager calculates the revenue according to (39) and records the current price, demand vector, and revenue value. The final solution in (42) is therefore chosen from all recorded iterations, rather than being determined only by the terminal price.

Algorithm 1 Distributed Iterative Pricing

1: Initialize the price as $p^{(0)} = \lambda$ and set $t = 0$.
2: Broadcast $p^{(t)}$ to all service requests.
3: Each service request i computes $b_i^*(p^{(t)})$ according to Section 5 and returns it to the manager.
4: The manager computes $R^{(t)}$ by (39) and stores $\left(p^{(t)}, \mathbf{b}^*(p^{(t)}), R^{(t)}\right)$.
5: **if** $\mathbf{b}^*(p^{(t)}) = (0, \ldots, 0)$ **then**
6: Terminate.
7: **else**
8: Update the price by (40), set $t \leftarrow t+1$, and repeat from Step 2.
9: **end if**
10: Output $p^\dagger$ and the corresponding $\mathbf{b}^\dagger$ according to (42).

This algorithm has a low information requirement and is suitable when service requests are unwilling to disclose their utility parameters. Its main limitation is that it requires repeated price broadcasting and response collection, and it does not guarantee the global optimum for an arbitrary step size λ. Since the algorithm evaluates only the discrete price sequence generated by the step size, an excessively large λ may skip a narrow high-revenue region and return only the best sampled price.

6.2. Genetic Algorithm Based on Backward Induction

When the communication resource manager can obtain the service-side parameters, the follower-side best responses in Section 5 can be evaluated directly for any candidate price. In this case, the pricing problem can be converted into a one-dimensional search over the price variable, and a genetic algorithm is adopted to obtain a more accurate approximate equilibrium.

For each service request i, define the effective upper bound of acceptable price as

$$\bar{p}_i = \begin{cases} \hat{p}_i, & B_i r_i \leq 2, \\ p_i^{\text{zero}}, & B_i r_i > 2, \end{cases} \tag{43}$$

and define the global search upper bound as

$$\bar{p} = \max_{i \in \mathcal{I}} \bar{p}_i. \tag{44}$$

Then, the feasible price interval for the genetic algorithm is

$$p \in (0, \bar{p}]. \tag{45}$$

Each chromosome encodes a candidate price p. Since the leader-side revenue is piecewise-defined and may contain multiple local maxima, the initial population is generated by uniform sampling over $(0, \bar{p}]$. For a chromosome with value p, the corresponding follower responses are computed by the backward-induction formulas in Section 5, and the fitness is defined as

$$F(p) = R\left(p, \mathbf{b}^*(p)\right). \tag{46}$$

Thus, individuals with higher revenue are assigned higher fitness.

Tournament selection is adopted to reduce the risk of premature convergence. Let $p^{(1)}$ and $p^{(2)}$ be two selected parent chromosomes, where $F(p^{(2)}) \geq F(p^{(1)})$. The offspring is generated by the directional crossover

$$p^{\text{child}} = p^{(1)} + \eta\left(p^{(2)} - p^{(1)}\right), \tag{47}$$

where $\eta \in (0, 1)$ is the crossover ratio. Following the original design, η is set to 0.4. A mutation operator is further introduced with mutation probability μ_m to maintain population diversity and help the search escape local optima. Following the original setting, μ_m is set to 0.025. In addition, an elitism strategy is used: the best individuals in the current generation are copied to the next generation, so that high-quality solutions are not lost during evolution.

Let $\mathcal{G}^{(n)}$ denote the population at generation n. The iterative procedure continues until the best individual remains unchanged for a prescribed number of generations. In the implementation adopted here, the algorithm stops when the best chromosome is unchanged for 10 consecutive generations. The final price returned by the algorithm is the chromosome with the highest fitness in the last generation. The procedure of the backward-induction-based genetic algorithm is summarized in Algorithm 2.

Algorithm 2 Genetic Algorithm Based on Backward Induction

1: Uniformly initialize a population of candidate prices over $(0, \bar{p}]$.
2: For each chromosome p, compute the follower-side response $\mathbf{b}^*(p)$ by the backward-induction formulas in Section 5.
3: Evaluate the fitness of each chromosome using (46).
4: Generate the next population by tournament selection, crossover using (47), mutation, and elitism.
5: **if** the best chromosome is unchanged for 10 consecutive generations **then**
6:     Terminate.
7: **else**
8:     Repeat from Step 2.
9: **end if**
10: Output the chromosome with the highest fitness, denoted by $p^\star_{\mathrm{GA}}$, together with its corresponding follower response $\mathbf{b}^*(p^\star_{\mathrm{GA}})$.

In Algorithm 2, each chromosome represents a candidate unit bandwidth price. For a given chromosome p, Step 2 computes the follower-side response vector $\mathbf{b}^*(p)$ by applying the backward-induction formulas derived in Section 5 to all service requests. Then, in Step 3, the obtained response vector is substituted into the leader-side revenue function, and the resulting revenue is used as the fitness value according to (46). Thus, the fitness evaluation reflects the revenue achieved by the communication resource manager under the candidate price and the corresponding follower-side demand response. Based on these fitness values, the tournament selection, crossover, mutation, and elitism operations in Step 4 are performed to generate the next population.

Compared with the distributed iterative algorithm, this method directly uses the analytical follower response derived in Section 5 and therefore provides a more refined search over the price space. It is suitable when the manager can access or estimate the service-side parameters. Its main limitation is the stronger information requirement. In summary, the distributed iterative algorithm is appropriate for privacy-sensitive scenarios with limited information sharing, whereas the genetic algorithm is more suitable for settings in which service-side parameters are available and higher solution accuracy is desired. The performance of both algorithms is evaluated in Section 7.

7. Simulation Results and Discussion

7.1. Simulation Setup

All simulations are conducted in MATLAB 2022b. Bandwidth is measured in Mbps, and the unit price p is expressed in price per Mbps. The payment of service request i is pb_i, and the provider revenue is $R = p\sum_{i\in\mathcal{I}} b_i$. The simulations are intended to evaluate model behavior and algorithm performance under the proposed pricing framework, rather than to claim general performance superiority over all existing pricing mechanisms.

This section addresses four questions. First, how do the service-side parameters E_i, B_i, and r_i affect utility, bandwidth demand, and pricing behavior? Second, how does the provider-side pricing behavior change under heterogeneous service requests? Third, how do the distributed iterative algorithm and the backward-induction-based genetic algorithm compare in convergence behavior and computational efficiency? Fourth, how do the pricing results change in multi-user and capacity-limited scenarios?

Unless otherwise stated, the distributed iterative algorithm uses the price step size specified in the corresponding experiment. For the genetic algorithm, the initial population is generated uniformly over the search interval, and the algorithm terminates when the best individual remains unchanged for 10 consecutive generations. The detailed settings used in the algorithm comparison are reported in Section 7.4.

7.2. Impact of User-Side Parameters

We first examine the effects of the service-side parameters in the utility model. The parameter E_i determines the maximum attainable benefit of service request i, B_i determines the minimum acceptable bandwidth demand, and r_i controls the return of additional bandwidth beyond the minimum acceptable demand. These three parameters jointly determine whether a service request accepts the announced price and how much bandwidth it purchases.

As shown in Figure 4, a larger E_i increases the attainable service-side utility under the same pricing condition. Since E_i is the upper bound of the benefit term, increasing E_i effectively lifts the utility surface and enlarges the positive-utility region. This implies a stronger willingness to remain active under higher prices. In addition, according to (20) and (23), both the critical marginal-benefit price $p_i^{\max}$ and the acceptance threshold $\hat{p}_i$ increase with E_i. Therefore, service requests with larger E_i are more likely to remain active at higher prices and to sustain larger purchased bandwidth once they are admitted.

Figure 5 shows that a larger B_i shifts the utility-effective region to a larger bandwidth level, reflecting a stricter service-side acceptance threshold. In economic terms, B_i determines the minimum bandwidth level from which resource purchase becomes meaningful. When B_i increases, the minimum acceptable operating point shifts to a larger bandwidth region, making the service request more sensitive to the announced price and more likely to reject insufficient allocations. Moreover, from (23), the acceptance threshold $\hat{p}_i = E_i/(2B_i)$ decreases as B_i increases. Hence, although a larger B_i corresponds to a higher minimum service requirement, it also narrows the price region in which the request is willing to remain active.

Figure 6 illustrates that r_i changes the curvature of the utility function and thus affects how quickly the marginal benefit of additional bandwidth saturates. A larger r_i makes the marginal gain of additional bandwidth saturate faster, while a smaller r_i implies that more bandwidth is needed before the service-side benefit approaches its upper bound. At the same time, (20) shows that $p_i^{\max} = E_i r_i/4$ increases with r_i, which means that the request can tolerate a larger marginal price at the minimum acceptable demand point. Therefore, r_i primarily affects the demand response beyond the minimum acceptable bandwidth level and plays an important role in shaping the local sensitivity of the purchased bandwidth to price.

Taken together, Figures 4–6 show that the three parameters affect follower behavior in different ways. This supports the use of (E_i, B_i, r_i) as heterogeneous demand descriptors in the proposed pricing model.

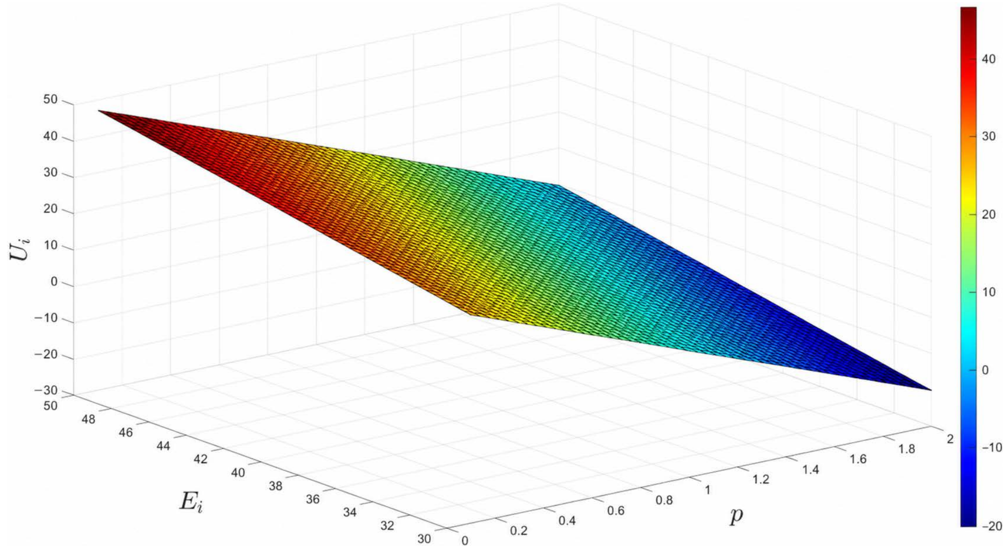

Figure 4. Impact of E_i on the service-side utility under the proposed pricing model.

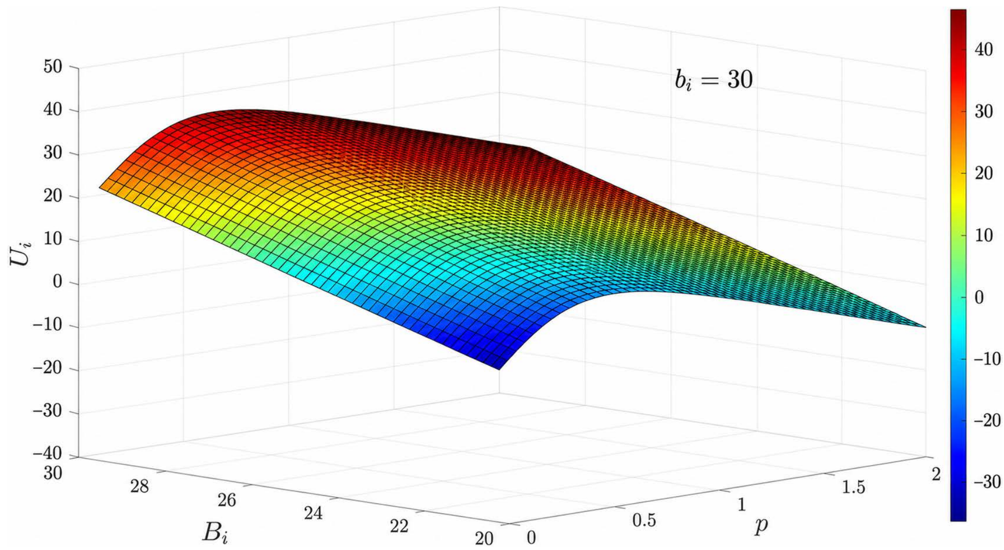

Figure 5. Impact of B_i on the service-side utility under the proposed pricing model.

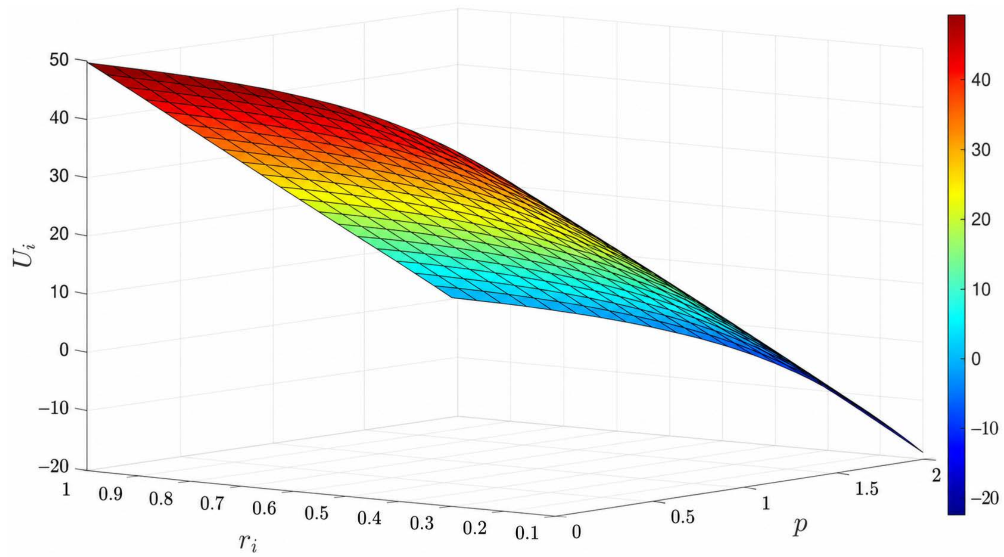

Figure 6. Impact of r_i on the service-side utility under the proposed pricing model.

7.3. Pricing Behavior Under Heterogeneous Users

As shown in Figure 7, larger E_i generally supports a higher price level because the corresponding service requests can tolerate larger payments while still maintaining positive utility. From the provider-side perspective, increasing E_i enlarges the price region in which the associated request remains active, so the demand reduction caused by price increases becomes less severe. This allows the provider to maintain a higher announced price before the demand of high-E_i requests collapses to zero. The figure also shows that the revenue-maximizing point is determined by the joint effect of price and admitted bandwidth, rather than by price alone. Therefore, a larger E_i not only raises the attainable utility of the service request, but also improves the provider-side flexibility in setting a profitable price.

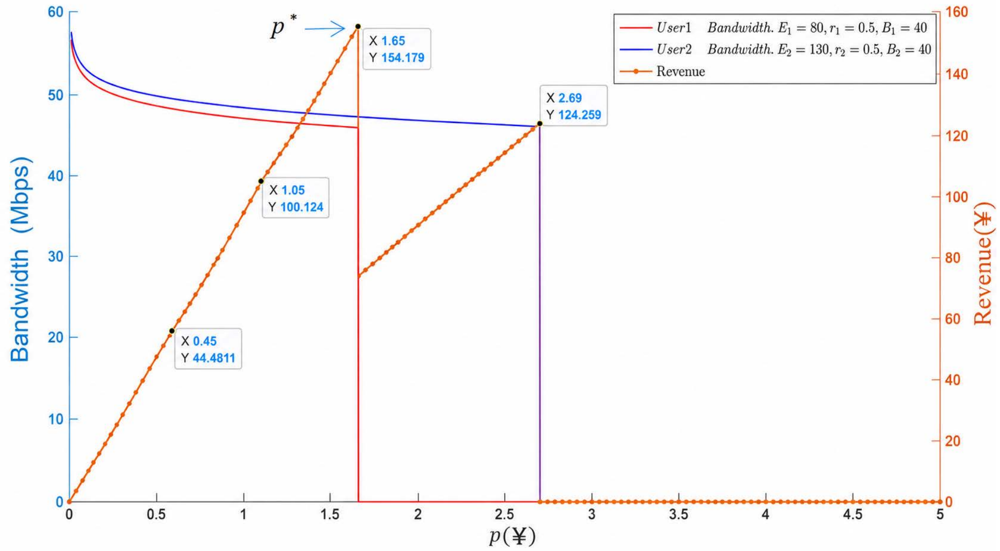

Figure 7. Pricing behavior under heterogeneous E_i. The asterisk it denotes the optimal/equilibrium value.

Figure 8 shows that the effect of B_i is more structural. A larger minimum acceptable bandwidth demand reduces the feasible response region and changes the points at which service requests leave the market. Compared with the case of varying E_i, changing B_i does not simply shift the price tolerance upward or downward; instead, it modifies the admission structure itself. In particular, when B_i is large, a request may remain inactive unless the available purchase level can satisfy its minimum service requirement, which makes the provider-side revenue curve more sensitive to the disappearance of individual requests. As a result, both the admitted demand profile and the final provider-side price can change significantly when heterogeneous B_i values are present.

Figure 9 indicates that the return factor r_i mainly changes the willingness to purchase bandwidth beyond the minimum acceptable level. Specifically, heterogeneous r_i values lead to different decay rates of bandwidth demand as the price increases, which means that the provider observes different demand elasticities from different requests. In the figure, this effect appears as different dropping patterns of the follower-side bandwidth curves and a corresponding change in the revenue-maximizing price. Therefore, unlike B_i, which mainly affects the acceptance threshold, r_i mainly reshapes the local response pattern after admission and thus changes how the provider balances price increase against aggregate demand loss.

Taken together, Figures 7–9 show that heterogeneous service attributes affect provider-side pricing through different mechanisms: E_i mainly enlarges the price-tolerant utility region, B_i changes the admission structure through the minimum acceptable demand, and r_i reshapes the post-admission demand elasticity. This explains why the provider-side revenue function becomes increasingly difficult to characterize exactly when heterogeneous requests coexist.

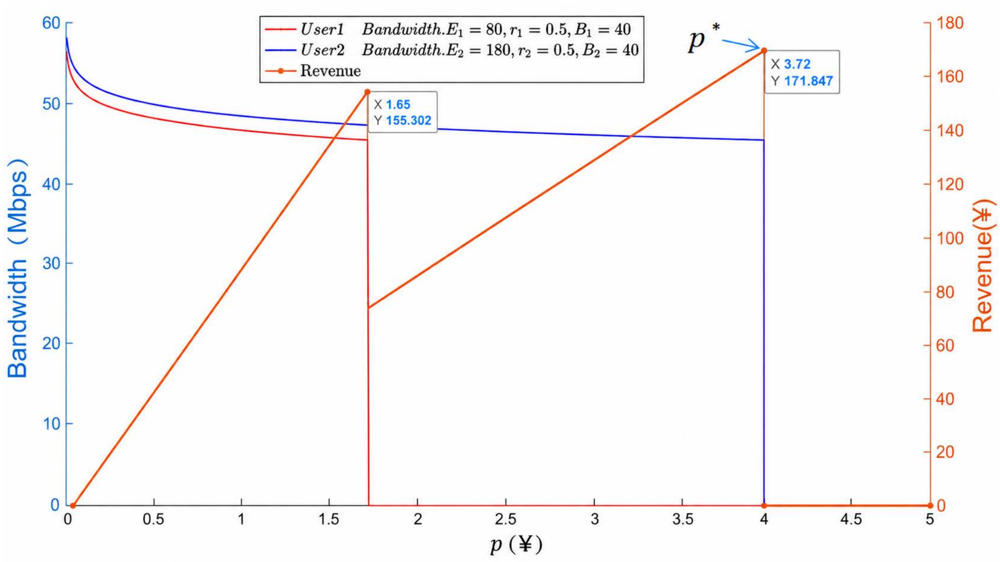

Figure 8. Pricing behavior under heterogeneous B_i. The asterisk it denotes the optimal/equilibrium value.

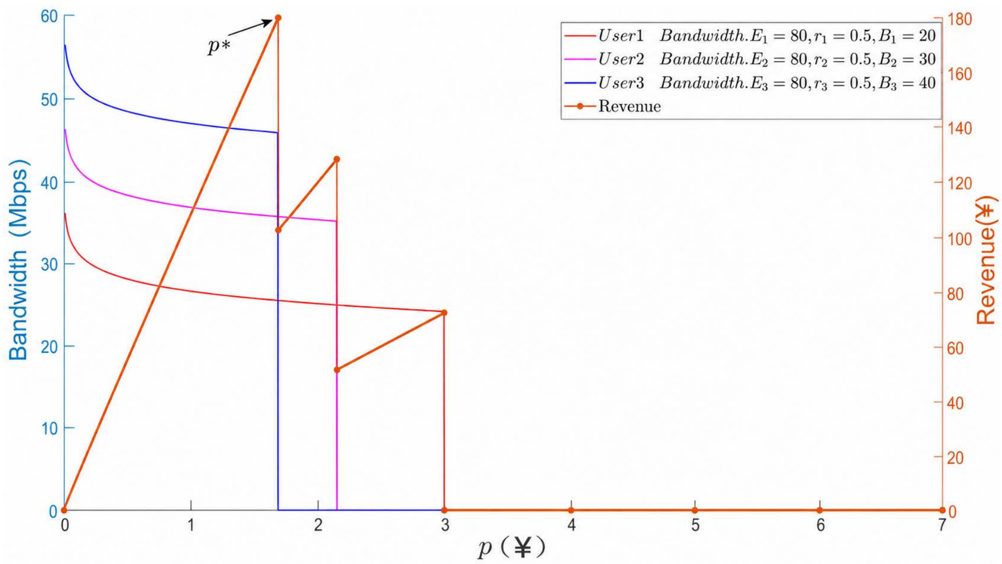

Figure 9. Pricing behavior under heterogeneous r_i. The asterisk it denotes the optimal/equilibrium value.

7.4. Performance of the Proposed Algorithms

We further evaluate the performance of the two proposed algorithms. The backward-induction-based genetic algorithm can directly use the analytical follower-side response derived in Section 5, whereas the distributed iterative algorithm only relies on repeated price broadcasting and response collection. Therefore, this subsection focuses on two aspects: the convergence behavior of the genetic algorithm and the computational cost of the two methods.

As shown in Figure 10, the best individual converges to a stable price value, while the population fitness gradually concentrates near the high-fitness region. This indicates that the proposed genetic algorithm is able to move the population toward a stable high-revenue region rather than oscillating over widely separated candidate solutions. In other words, the evolutionary process does not merely preserve an isolated good individual; it also improves the overall population quality as the generations proceed.

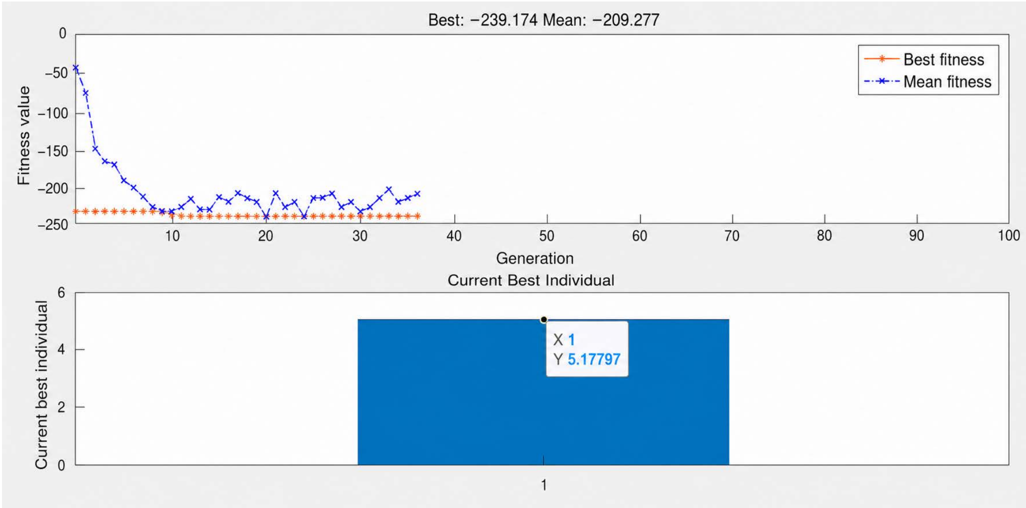

Figure 10. Best individual and population fitness evolution.

Figure 11 further shows that the best fitness stabilizes after several generations, indicating effective convergence of the proposed genetic algorithm. A noticeable improvement is obtained in the early generations, after which the fitness variation becomes much smaller. This behavior suggests that the search process first identifies the promising price region quickly and then performs local refinement around that region. Such a convergence pattern is consistent with the piecewise structure of the provider-side revenue function derived in Section 5.

Table 2 reports the runtime comparison over repeated test instances. The distributed iterative algorithm requires an average runtime of 53.6701 s, whereas the genetic algorithm requires an average runtime of 12.266 s. Therefore, in the reported experiments, the genetic algorithm reduces the runtime by approximately a factor of four while maintaining stable convergence behavior. In addition, the average number of convergence generations is 28.6, which is consistent with the stabilization trend observed in Figures 10 and 11.

Table 2. Performance comparison of the proposed algorithms.

Trial	Distributed Iterative Algorithm (s)	Genetic Algorithm (s)	Convergence Generations
1	54.329	12.273	14
2	53.119	12.339	31
3	56.455	12.555	28
4	56.855	10.786	27
5	55.172	13.554	35
6	51.653	12.476	31
7	51.835	12.143	29
8	51.227	14.604	35
9	53.203	11.730	30
10	52.853	10.200	26
Average	53.670	12.266	28.6

These results show that the backward-induction-based genetic algorithm provides a more efficient search mechanism when the service-side parameters are available. By contrast, the distributed iterative algorithm remains useful in privacy-sensitive settings, but its computational cost is higher because it relies on repeated price broadcasting and response collection over a discretized price grid. Therefore, the two algorithms are appropriate for different operational conditions: the distributed iterative algorithm is more suitable when private utility information is unavailable, whereas the genetic algorithm is more attractive when stronger information availability allows faster equilibrium search.

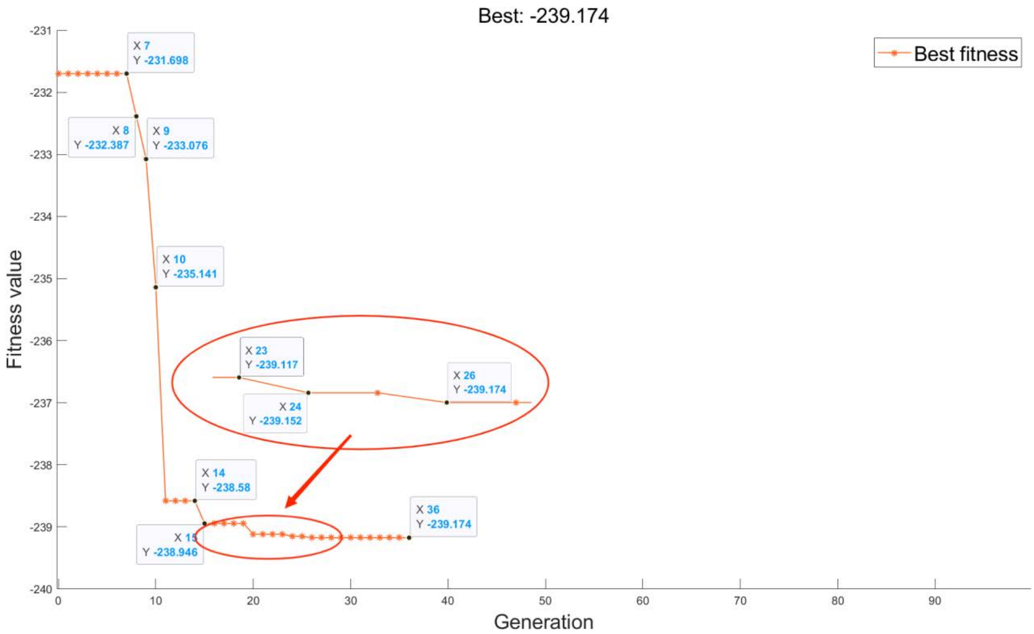

Figure 11. Evolution of the best fitness across generations.

7.5. Multi-User and Capacity-Limited Scenarios

We finally examine larger multi-user and capacity-limited scenarios. In the multi-user experiment, the service-request parameters are generated randomly, so that the resulting demand profiles cover diverse combinations of minimum acceptable bandwidth demand, attainable benefit, and additional-bandwidth return.

As shown in Figure 12, the provider-side price gradually stabilizes as the number of service requests increases. This behavior indicates that the aggregate demand profile becomes more regular in large-population scenarios. A key reason is that, as the user population grows, the proportion of requests with medium-level bandwidth requirements becomes more stable, so excessively aggressive pricing would cause the provider to lose a large portion of otherwise profitable demand. As a result, the revenue-maximizing price no longer fluctuates strongly with individual user attributes and instead converges toward a relatively stable level.

Figure 13 shows that, in the reported simulations, the average revenue contributed by each service request varies within a relatively narrow range, whereas the total provider revenue increases with the number of participating requests. This indicates that the gain in total revenue mainly comes from the enlargement of the admitted user population rather than from extracting substantially higher revenue from each individual request. In this sense, the multi-user results suggest that moderate pricing can be more beneficial than aggressive pricing in scenarios with large numbers of users, because a lower but acceptable price helps preserve a broader demand base and leads to more stable aggregate revenue.

We next consider the capacity-limited case. Let C denote the total available bandwidth capacity. If

$$\sum_{i \in \mathcal{I}} b_i^*(p) > C, \tag{48}$$

the provider admits only a subset of service requests so as to maximize its revenue under the capacity constraint. This exhaustive subset evaluation is used only for small-scale validation and for illustrating the capacity-threshold effect caused by minimum acceptable bandwidth demands. Its worst-case computational complexity grows exponentially with the number of service requests, and therefore it is not intended for large-scale online implementation.

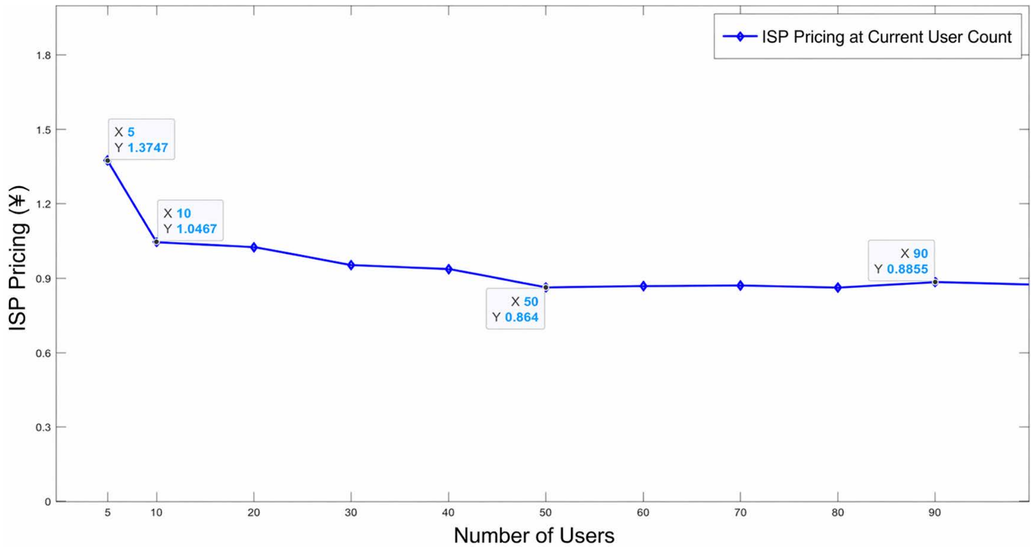

Figure 12. Provider-side pricing behavior in the multi-user scenario.

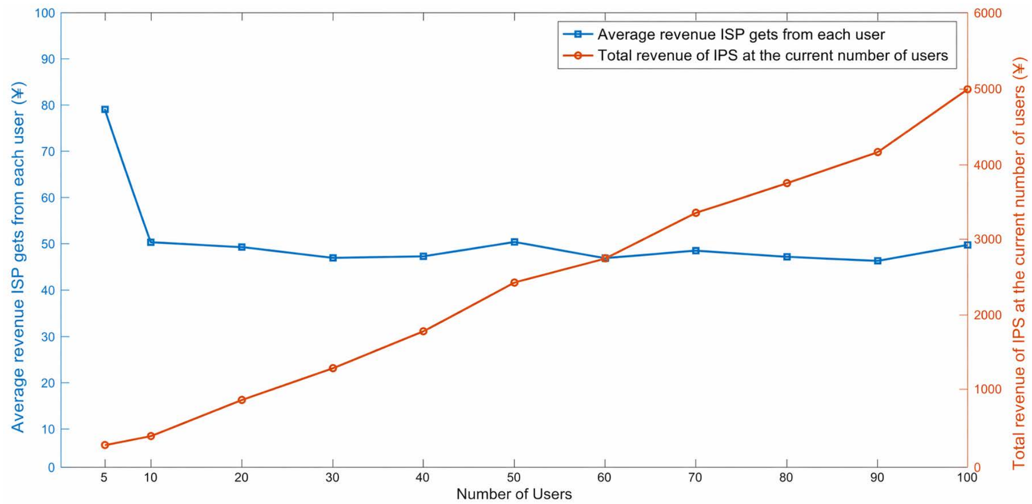

Figure 13. Average revenue per service request and total provider revenue in the multi-user scenario.

Figure 14 shows that provider revenue and the selected price change discretely with network capacity when minimum acceptable bandwidth demands are considered. Capacity expansion changes not only the feasible admitted demand, but also the price selected by the provider. This is because the minimum acceptable bandwidth demand prevents the provider from using arbitrarily small residual capacity to serve additional requests. Therefore, the effective revenue is determined by both the announced price and the set of users whose minimum requirements can be jointly satisfied under the current capacity limit.

As shown in Figure 15, a small increase in capacity may produce a sharp revenue gain when the additional bandwidth becomes sufficient to admit one more service request whose minimum acceptable demand was previously unmet. This result reflects a threshold effect induced by minimum-demand constraints: once the available capacity crosses a critical boundary, the feasible admission set changes, and the provider may switch to a more profitable allocation strategy. These results indicate that, under capacity constraints, the provider-side pricing decision is jointly shaped by aggregate demand, admission feasibility, and the minimum acceptable bandwidth requirements of heterogeneous service requests.

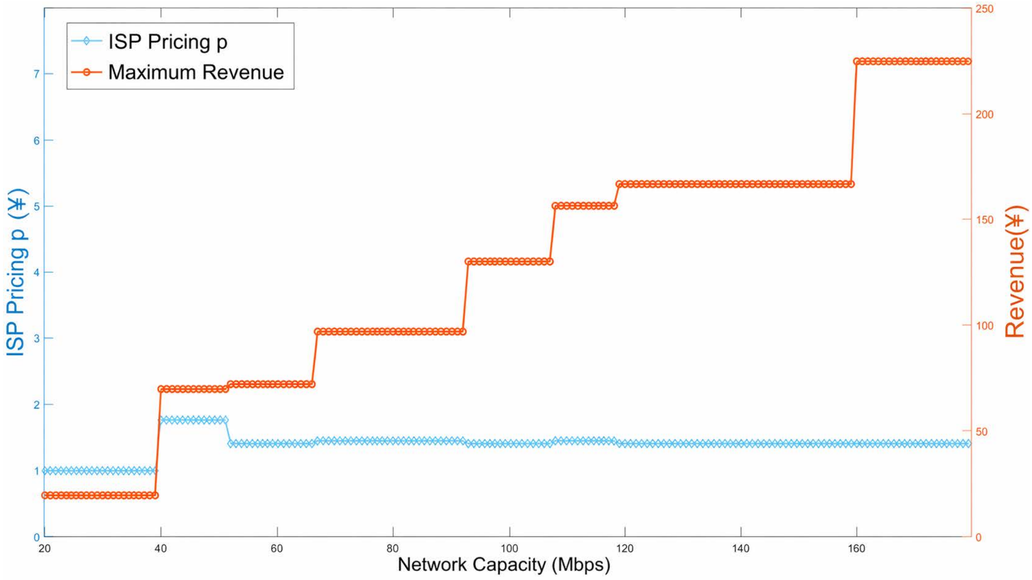

Figure 14. Provider revenue and price under limited network capacity.

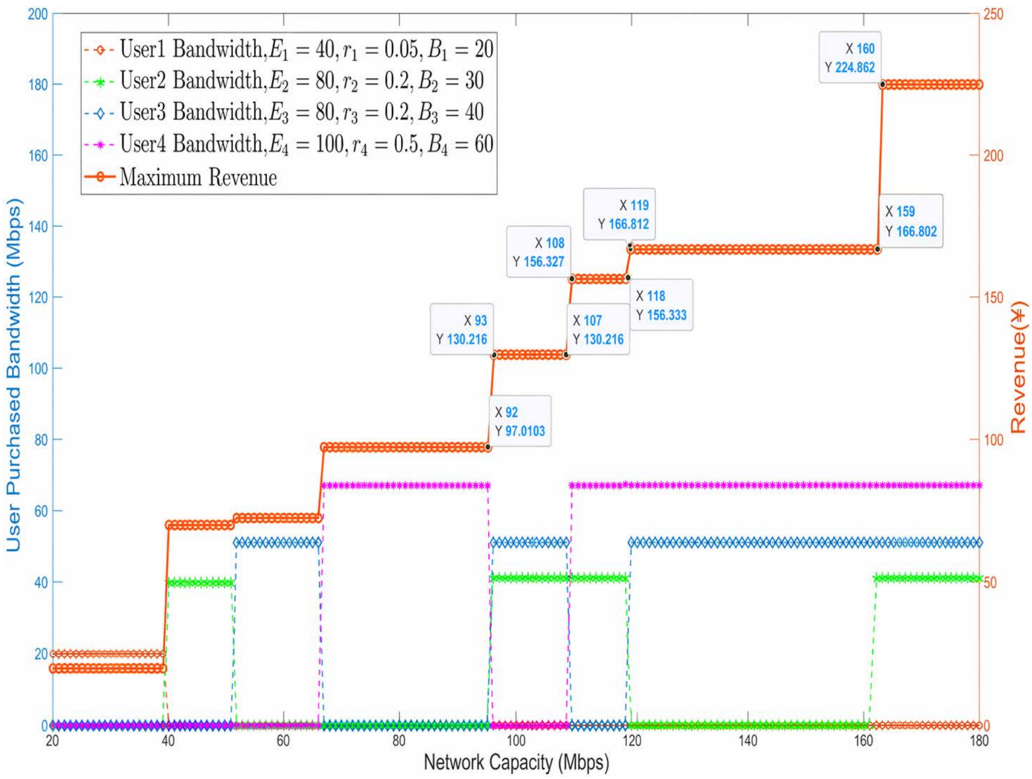

Figure 15. Provider revenue and resource allocation under limited network capacity.

It should also be noted that, because the current provider-side objective focuses on revenue maximization, the admitted subset under a capacity constraint is not necessarily fairness-preserving. A request with a high minimum acceptable bandwidth demand may be excluded if its admission consumes a large amount of capacity but provides a lower revenue contribution than other feasible request combinations. In the unconstrained case, the provider does not explicitly exclude requests, because each request independently decides whether to participate according to its own utility under the announced price. However, under limited capacity, the revenue-oriented admission rule may disadvantage requests with large minimum bandwidth requirements. Fairness-aware admission constraints, service-priority rules, or minimum service guarantees can be incorporated into the provider-side problem in an extended model.

In addition, the current model responds to traffic variation through price recomputation across pricing intervals, but it does not explicitly model sudden traffic spikes or bursty demand; burst-aware or robust dynamic pricing will be considered in future work.

8. Conclusions

This paper studied demand-aware dynamic pricing in an SDN-enabled resource-allocable communication network motivated by smart grid-inspired service scenarios. A pricing-oriented abstraction was first established to describe how service requests observe network-state information and adjust their bandwidth purchases in response to the announced unit price. Based on this abstraction, a Stackelberg game was formulated to characterize the interaction between a communication resource manager and multiple service requests, where the minimum acceptable bandwidth demand of each request was explicitly incorporated into the utility model to reflect service-side acceptance behavior. The equilibrium properties of the proposed game were then analyzed, the follower-side best response was derived through backward induction, and two approximate solution methods, namely, a distributed iterative algorithm and a backward-induction-based genetic algorithm, were developed for different information settings. Simulation results further showed how the service-side parameters affect bandwidth demand and provider pricing, and evaluated the proposed methods in heterogeneous-user, multi-user, and capacity-limited scenarios.

The current model still focuses on bandwidth-oriented pricing and does not explicitly incorporate delay, reliability, packet loss, or other QoS requirements into the utility and pricing functions. Therefore, compared with a multi-dimensional QoS-aware pricing approach, the proposed model characterizes the pricing problem mainly from the bandwidth dimension and does not yet capture the tradeoffs among multiple service-quality attributes. In addition, the proposed pricing mechanism has been evaluated through model-based simulations, but has not yet been validated in a real communication environment. Future work will therefore extend the model to multi-dimensional QoS-aware pricing and further evaluate it in practical deployment scenarios.

Author Contributions: Conceptualization, X.F. and H.G.; methodology, H.G. and B.G.; investigation, B.G.; resources, X.W. and J.D.; data curation, X.W., J.D. and J.L.; writing—original draft preparation, J.L. and Q.G.; writing—review and editing, Q.G. and W.W.; visualization, J.D. and Q.G.; supervision, J.L.; project administration, X.F. All authors have read and agreed to the published version of the manuscript.

Funding: The authors declare that this study received funding from the Science and Technology Project of China Southern Power Grid Co., Ltd., grant number 030100KC23110063 (GDKJXM20231279). The funder was not involved in the study design, collection, analysis, interpretation of data, the writing of this article, or the decision to submit it for publication.

Data Availability Statement: The original contributions presented in this study are included in the article Further inquiries can be directed to the corresponding author.

Acknowledgments: The authors would like to thank the editor and all reviewers for their valuable comments and efforts on this article.

Conflicts of Interest: Authors Xingxing Feng, Haitong Gu, Bin Guo, Xiaoqiang Wu, Jun Dong, and Jingbo Lin were employed by the company Guangzhou Power Supply Bureau, Guangdong Power Grid Co., Ltd. The remaining authors declare that the research was conducted in the absence of any commercial or financial relationships that could be construed as potential conflicts of interest.

References

1. Porambage, P.; Okwuibe, J.; Liyanage, M.; Ylianttila, M.; Taleb, T. Survey on multi-access edge computing for Internet of Things realization. *IEEE Commun. Surv. Tuts.* **2018**, *20*, 2961–2991. [CrossRef]
2. Suhaimy, N.; Radzi, N.A.M.; Ahmad, W.S.H.M.W.; Azmi, K.H.M.; Hannan, M.A. Current and future communication solutions for smart grids: A review. *IEEE Access* **2022**, *10*, 43639–43668. [CrossRef]
3. Wen, M.H.F.; Leung, K.-C.; Li, V.O.K.; He, X.; Kuo, C.-C.J. A survey on smart grid communication system. *APSIPA Trans. Signal Inf. Process.* **2015**, *4*, e5. [CrossRef]
4. Citroni, R.; Mangini, F.; Frezza, F. Efficient integration of ultra-low power techniques and energy harvesting in self-sufficient devices: A comprehensive overview of current progress and future directions. *Sensors* **2024**, *24*, 4471. [CrossRef] [PubMed]
5. Kreutz, D.; Ramos, F.M.V.; Verissimo, P.; Rothenberg, C.E.; Azodolmolky, S.; Uhlig, S. Software-defined networking: A comprehensive survey. *Proc. IEEE* **2015**, *103*, 14–76. [CrossRef]
6. McKeown, N.; Anderson, T.; Balakrishnan, H.; Parulkar, G.; Peterson, L.; Rexford, J.; Shenker, S.; Turner, J. OpenFlow: Enabling innovation in campus networks. *SIGCOMM Comput. Commun. Rev.* **2008**, *38*, 69–74. [CrossRef]
7. Nunes, B.A.A.; Mendonca, M.; Nguyen, X.-N.; Obraczka, K.; Turletti, T. A survey of software-defined networking: Past, present, and future of programmable networks. *IEEE Commun. Surv. Tuts.* **2014**, *16*, 1617–1634. [CrossRef]
8. Caba, C.; Soler, J. SDN-based QoS aware network service provisioning. In *Mobile, Secure, and Programmable Networking*; Lecture Notes in Computer Science; Springer: Cham, Switzerland, 2015; Volume 9395, pp. 119–133.
9. Bagaa, M.; Dutra, D.L.C.; Taleb, T.; Samdanis, K. On SDN-driven network optimization and QoS aware routing using multiple paths. *IEEE Trans. Wirel. Commun.* **2020**, *19*, 4700–4714. [CrossRef]
10. Karakus, M.; Durresi, A. Quality of service (QoS) in software-defined networking (SDN): A survey. *J. Netw. Comput. Appl.* **2017**, *80*, 200–218. [CrossRef]
11. Shu, Z.; Taleb, T. A novel QoS framework for network slicing in 5G and beyond networks based on SDN and NFV. *IEEE Netw.* **2020**, *34*, 256–263. [CrossRef]
12. Abbou, A.N.; Taleb, T.; Song, J.S. A software-defined queuing framework for QoS provisioning in 5G and beyond mobile systems. *IEEE Netw.* **2021**, *35*, 168–173. [CrossRef]
13. Messaoudi, S.; Ksentini, A.; Bonnet, C. SDN framework for QoS provisioning and latency guarantee in 5G and beyond. In Proceedings of the IEEE 20th Consumer Communications & Networking Conference (CCNC), Las Vegas, NV, USA, 8–11 January 2023; pp. 1–6.
14. Gizelis, C.A.; Vergados, D.D. A survey of pricing schemes in wireless networks. *IEEE Commun. Surv. Tuts.* **2011**, *13*, 126–145. [CrossRef]
15. D'Oro, S.; Galluccio, L.; Mertikopoulos, P.; Morabito, G.; Palazzo, S. Auction-based resource allocation in OpenFlow multi-tenant networks. *Comput. Netw.* **2017**, *115*, 29–41. [CrossRef]
16. Basar, T.; Srikant, R. A Stackelberg network game with a large number of followers. *J. Optim. Theory Appl.* **2002**, *115*, 479–490. [CrossRef]
17. Tong, Z.; Deng, X.; Mei, J.; Dai, L.; Li, K.; Li, K. Stackelberg game-based task offloading and pricing with computing capacity constraint in mobile edge computing. *J. Syst. Archit.* **2023**, *137*, 102847. [CrossRef]
18. Holland, J.H. *Adaptation in Natural and Artificial Systems: An Introductory Analysis with Applications to Biology, Control, and Artificial Intelligence*; MIT Press: Cambridge, MA, USA, 1992.
19. Rosen, J.B. Existence and uniqueness of equilibrium points for concave n-person games. *Econometrica* **1965**, *33*, 520–534. [CrossRef]
20. Yiakoumis, Y.; Katti, S.; Huang, T.Y.; McKeown, N.; Yap, K.K.; Johari, R. Putting home users in charge of their network. In Proceedings of the 2012 ACM Conference on Ubiquitous Computing, Pittsburgh, PA, USA, 5–8 September 2012; pp. 1114–1119.
21. Kumar, H.; Gharakheili, H.H.; Sivaraman, V. User control of quality of experience in home networks using SDN. In Proceedings of the 2013 IEEE International Conference on Advanced Networks and Telecommunications Systems (ANTS), Kattankulathur, India, 15–18 December 2013; pp. 1–6.
22. Ferguson, A.D.; Guha, A.; Liang, C.; Fonseca, R.; Krishnamurthi, S. Participatory networking: An API for application control of SDNs. *ACM SIGCOMM Comput. Commun. Rev.* **2013**, *43*, 327–338. [CrossRef]
23. Puspita, F.M.; Seman, K.; Taib, B.M. The improved models of internet pricing scheme of multi-service multi-link networks with various capacity links. In *Advanced Computer and Communication Engineering Technology: Proceedings of the 1st International Conference on Communication and Computer Engineering*; Springer International Publishing: Cham, Switzerland, 2014; pp. 1–6.
24. Hussein, N.; Seman, K.; Puspita, F.M.; Rahim, K.A.; Sahrim, M.A. Improved model of internet pricing incentive mechanism based on multi bottleneck links in multi QoS networks. In Proceedings of the 2021 International Conference on Electrical, Communication, and Computer Engineering (ICECCE), Kuala Lumpur, Malaysia, 12–13 June 2021; pp. 1–5.

25. Zekri, M.; Hadji, M.; Jouaber, B.; Zeghlache, D. A Nash-Stackelberg approach for network pricing, revenue maximization and vertical handover decision making. In Proceedings of the 2011 IEEE 36th Conference on Local Computer Networks, Bonn, Germany, 4–7 October 2011; pp. 622–629.
26. Fan, Y.; Wang, L.; Wu, W.; Du, D. Cloud/edge computing resource allocation and pricing for mobile blockchain: An iterative greedy and search approach. *IEEE Trans. Comput. Soc. Syst.* **2021**, *8*, 451–463. [CrossRef]